Available online at www.sciencedirect.com
ScienceDirect
Thermochimica Acta 450 (2006) 47–55
thermochimica acta
www.elsevier.com/locate/tca

The use of advanced calorimetric techniques in polymer synthesis and characterization

Jean-Pierre E. Grolier [a,*], Florin Dan [b]

[a] *Laboratory of Thermodynamics of Solutions and Polymers, Blaise Pascal University, 24 des Landais Avenue, 63177 Aubière, France*
[b] *Department of Macromolecular Chemistry, "Gh. Asachi" Technical University, 700050 Iasi, Romania*

Available online 31 July 2006

Abstract

Progress in the understanding of polymer synthesis, including the crucial step of initiation and undesired side reactions, and in characterization of polymers, especially their thermal behaviour, are directly related to advances in calorimetric technologies.

In polymer synthesis, since polymerization reactions are highly exothermic, reaction calorimetry (RC) is an appropriate technique for on-line process monitoring. Measurements are non-invasive, rapid, and straightforward. Viscosity increase and fouling at the reactor wall are typical features of many polymerizations. The global heat transfer coefficient, *UA*, also changes drastically when viscosity increases and affects the accuracy of calorimetric measurements. Our approach was focused on oscillating temperature calorimetry (TOC). Reactions were performed with two different reaction calorimeters, i.e. an isoperibolic calorimeter and a Calvet-type high sensitivity differential calorimeter, respectively. Special attention was paid to the interpretation of the measured signals to obtain reliable calorimetric data. The evolution of heat transfer coefficient was followed by performing two Joule effect calibration experiments, before and after the reaction, and the two values interpolated to obtain the desired profile of *UA*. A differentiation method based on the convolution of the measured heat flow by the generated one was used for determining the time constants and deconvoluting the measured heat flow.

With respect to polymer characterization, pressure-controlled scanning calorimetry, also called scanning transitiometry, is now a well established technique. The transitiometer was coupled to an ultracryostat to work at low temperature. The assembly was used to follow the pressure effect on phase change phenomena such as fusion/crystallization and glass transition temperature T_g of low molecular weight substances or high molecular weight polymers.

Keywords: Reaction calorimetry; Polymerization; Heat of reaction; Scanning transitiometry; Low temperature–high pressure; Phase change

1. Introduction

To identify optimal operating conditions of a chemical process, knowledge of kinetic and thermodynamic parameters for the most important main and side reactions are needed. A conventional method for investigating a reaction during process development is reaction calorimetry (RC) [1]. RC is the technique accepted as the most powerful way to study the process in near-to-the-industrial conditions, allowing a wide spectrum of operation conditions and measurements. The main driving force for developing process oriented calorimetric instruments was the evolution of electronic hardware, which made measurements easily possible on a (non-micro) laboratory scale [2].

A small-scale isoperibolic calorimeter was used for studying polymerization processes. In the isoperibolic mode the surroundings of the reaction mass (usually a jacket) are maintained at constant temperature. Exothermic or endothermic changes will produce a temperature increase or decrease in the reactor. The basic equation of RC is the heat balance of an exothermic reactor with external cooling jacket, under the hypothesis of perfect mixing in the reactor and in the jacket:

$$C_P \frac{dT_r}{dt} = UA(T_j - T_r) + Q_{chem} + Q_{loss} + P_{stirrer} \quad (1)$$

In Eq. (1) *UA* is the global heat transfer coefficient multiplied by heat transfer area, $W\,K^{-1}$. In the simplest case *UA* is assumed as constant and is obtained by carrying out an initial calibration experiment with a calibration heater. When the heat loss, Q_{loss}, and the power dissipated by the stirrer, $P_{stirrer}$, are known or negligible, Eq. (1) allows the evaluation of the heat of reaction

* Corresponding author. Tel.: +33 473 407186; fax: +33 473 407185.
E-mail address: J-Pierre.Grolier@univ-bpclermont.fr (J.-P.E. Grolier).

0040-6031/$ – see front matter © 2006 Elsevier B.V. All rights reserved.
doi:10.1016/j.tca.2006.07.016

in isothermal conditions [3]. However, strong variations of UA are frequently observed in polymerization reactions, due to an increase of reaction mass viscosity, and in biotechnology, where many fermentation processes are accompanied by a change in broth viscosity with time [4]. The increase in viscosity during polymerization is almost negligible in suspension and moderate in heterogeneous bulk polymerizations but significant changes occur in homogeneous bulk or solution polymerization [5]. This is why the homogeneous solution polymerization of acrylamide (AM) was chosen as model to illustrate the performances and the limits of RC. Special attention was paid to the interpretation of the measured signals in order to achieve reliable calorimetric data. The evolution of the heat transfer coefficient was followed by performing two calibration experiments, before and after the reaction; the two values of the heat transfer coefficient are subsequently interpolated, by obtaining the desired $UA(t)$ profile. In addition, a differentiation method based on the convolution of the measured heat flow by the generated one was used for determining the time constants and deconvoluting the measured heat flow. Another objective of this part is to develop temperature oscillation calorimetry (TOC), particularly in a small volume reactor (9 ml) in a Calvet-type differential calorimeter. The aim of this calorimetric technique is to obtain on-line the heat balance of the reaction mass during a chemical reaction, i.e. heat of reaction and heat transfer coefficient.

The second part of this work deals with the effect of pressure on phase transitions, particularly at low temperatures. Phase transitions are very important in industrial practice since the ignorance of a phase diagram, particularly at extreme conditions of pressure, temperature, and of chemical reactivity, is a limiting factor to the development of industrial processes [6]. When the goal is to investigate the pressure effects on the physical properties of compounds the calorimetric set-up must be adapted by adding a high-pressure line, up to 500 MPa [7]. Introducing pressure as an additional variable in the thermal analysis gives additional insight into the behaviour of such systems and a better understanding of their thermodynamics. The experimental setup was adapted by connecting the calorimetric block to a cooling/heating circulating system to extend the working temperature interval to −80 °C. Selected results of investigations concerning mercury fusion and glass transition temperature of some polymeric materials, all at high pressure, are given. This serves to illustrate the performance of scanning transitiometry in following phase change phenomena at low temperatures. Mercury was chosen as a model substance to illustrate the pressure effect on the first order phase transition since it is often used as a pressurizing fluid due to its chemical inertness and very suitable and well-known thermomechanical coefficients. Under conditions of normal pressure its melting temperature is −38.83 °C, but this temperature increases with pressure and special precautions must be taken in using it as pressurizing fluid at low temperature. On the other hand, the glass transition temperature of a polymer is a most important property because it determines the range of temperatures for processing and the range for applications. This temperature is the boundary between a low temperature, stiff, glassy state and high temperature rubbery state (due to the onset of long-range coordinated motion). In polymers, the glassy state can be achieved in two different routes by slowing down the dynamics of the molecular motion: i.e. by lowering the temperature rapidly enough below the glass transition temperature, T_g, or alternatively by elevating pressure above the glass transition pressure, P_g, at a constant temperature [8]. Pressure is one of the crucial parameters for the glass transition process, and the pressure effect on the structural relaxation and glass transition of amorphous solids is vital for understanding the nature of glass transition. Some examples concerning the pressure effect of the T_g of vulcanized rubbers are given in the last part of this work.

2. Experimental part

2.1. Chemicals

Acrylamide (AM), potassium permanganate, potassium persulfate, ascorbic acid and oxalic acid, used for polymerizations, were provided by Fluka Chemika, France and were used without further purification.

Propyl alcohol p.a. with purity >99.5 mol%, used as pressurizing fluid, was provided by (Fine Chemicals) Acros Organics France. It was distilled at atmospheric pressure, under nitrogen atmosphere, prior to use. Mercury was provided by Fluka Chemika, France, and used without further purification. The vulcanized rubber used in this study were a poly(butadiene-co-styrene) rubber with T_g of −50 °C at atmospheric pressure (determined with a Mettler Toledo DSC 821^e apparatus at 5 K min^{-1}).

2.2. Calorimeters

The reaction calorimeter is depicted in Fig. 1(a). The reactor is a 100 ml flask with a jacket and a lid with five ports. The flask jacket is connected to a thermostatic bath whose temperature is maintained within ±0.1 °C with a Vertex (model V9610) PID controller. One temperature sensor (Pt100) is placed in the reactor and two more at the jacket inlet and outlet, respectively. An additional J-type thermocouple (1 mm external diameter) is placed in the space between the lid and the liquid's surface. As the detail of Fig. 1(a) shows, the thermocouple is in intimate contact with the feeding tube and consequently with liquid containing the initiator solution. Since, the temperature of added liquid is usually below the reaction temperature, the decrease of temperature to the thermocouple serves as trigger for the start of reaction as well as to correct the Q_{Chem} by the heat exchanged with the reaction mass during reagent addition, Q_{Doss} in Eq. (1). The reactor also holds the calibration heater (15 Ω) powered by a 30 V/1 A power supply via a power amplifier connected to one of the analog outputs of the data acquisition board (a PCI-441D model from Datel Inc., USA). A LabVIEW® (National Instruments) program selects the voltage applied to the resistor during the pre-established calibration periods. In semibatch operation mode the reagent is fed over a period with a peristaltic pump (MasterFlex C/L, Barnant Company, USA) with a pre-calibrated feeding rate. The duration of feed is controlled by the software through a computer controlled relay. The whole application is

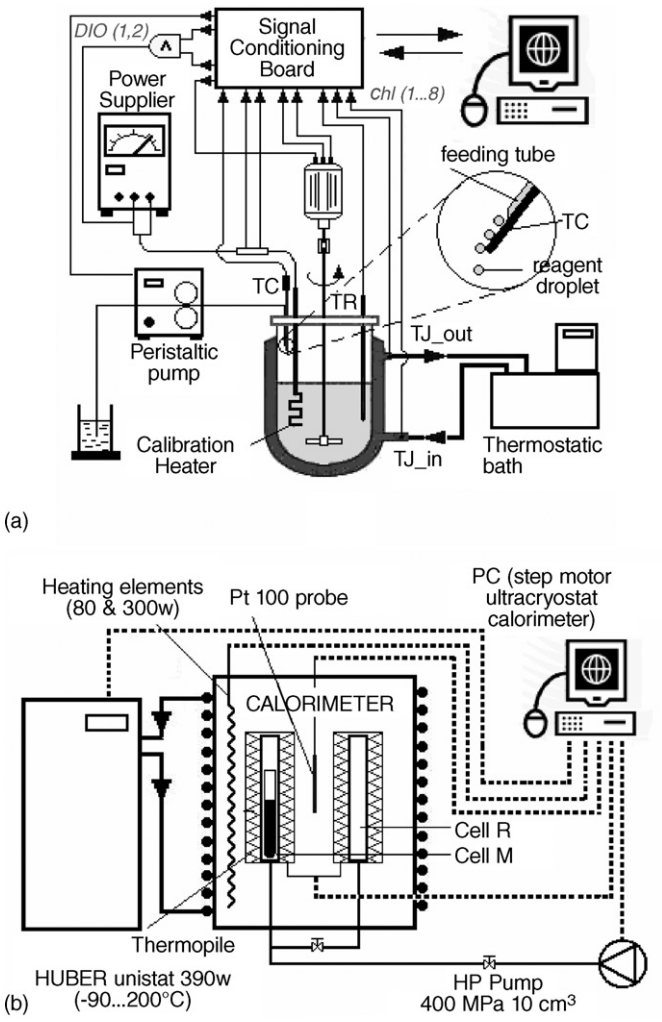

Fig. 1. Schematic view of isoperibolic calorimeter (a) and of the scanning transitiometer–cryostat (b). In the right hand part of scheme (a) a detail of the assembly thermocouple-feeding tube used as trigger for the zero moment of polymerization is given.

controlled by a single LabVIEW program. The program allows direct interaction to all devices connected to the system as well as automatic handling of a pre-defined recipe. The main task of the LabVIEW program is to acquire the data of all sensors and devices as well as to control the stirrer speed and the power dissipated by the calibration heater. Both tasks are performed by the same PCI-441D precision sensor input and multi-functional I/O board. Details concerning the signal conditioning board and the treatment of different signals acquired by the computer are given elsewhere [9]. The two analog outputs are used to control the stirrer speed and the power dissipated by the calibration heater, respectively.

A schematic view of the transitiometer–ultracryostat is given in Fig. 1(b). It consists of a BGR-Tech scanning transitiometer connected to a Hüber unistat, model 390w. The connection between the cryostat and the heating–cooling shield of the calorimetric block is made via two flexible thermoisolated hoses.

The transitiometer itself is constructed as a twin calorimeter with a variable operating volume. It is equipped with high-pressure vessels, a *pVT* system, and LabVIEW-based virtual instrument (VI) software. Two cylindrical calorimetric detectors ($\phi = 17$ mm, $l = 80$ mm) each made from 622 thermocouples (chromel–alumel) are mounted differentially and connected to a nanovolt amplifier, which functions as a non-inverting amplifier, whose gain is given by an external resistance (with 0.1% precision). The calorimetric detectors are placed in a metallic block, the temperature of which is directly controlled with a digital feedback loop of 22 bits resolution ($\sim 10^{-4}$ K), being part of the transitiometer software. The calorimetric block is surrounded by a heating–cooling jacket, which is connected to the cryostat. In addition, it is embedded in an electrically heated shield. The temperature difference between the block and the heating–cooling shield is set to a constant value (5, 10, 20, or 30 K) and is controlled by an analogue controller. The temperature measurements, both absolute and differential, are performed with calibrated 100 Ω Pt sensors; the Pt100 temperature sensor is placed between the sample and the reference cell. The heaters are homogeneously embedded on the outer surfaces of both the calorimetric block and the heating–cooling shield. The whole assembly is placed in thermal insulation enclosed in a stainless steel body and placed on a stand, which permits moving the calorimeter up and down over the calorimetric vessels. When performing measurements near 0 °C or below, dry air is pumped through the apparatus to prevent condensation of water vapour. A more detailed scheme of the hole assembly is given in Ref. [10]. The variable volume is realized with a step-motor driven piston pump. The resolution of the volume detection is ca. 5.24×10^{-6} cm^3 per step, as it was found by the measurement of the piston displacement for given numbers of steps, and the total variable volume is 9 cm^3. The calorimeter block can be lifted to load the sample into the cell, or for cleaning. The pressure sensors are connected close to the piston pump. Pressure can be detected with a precision of ±4 kPa.

The Hüber cryostat/thermostat connected to the calorimeter can be operated from −90 to 200 °C, with temperature stability at −10 °C of 0.02 K and cooling power at 0, −20, −40, −60 and −80 °C of 5.2, 5, 4.2, 3.1, and 0.9 kW, respectively. The maximum delivery of circulating pump is 40 l/min and the maximal delivery pressure is 1.5 bar. The cryostat is microprocessor controllable and equipped with an RS232 interface. The cryostat is PC-controlled thanks to a Labwordsoft® 3.01 graphical software. The software allows to build the temperature program (up to 99 sequences), controls the temperature with high accuracy, and performs data acquisition into a file, with a selectable frequency.

When the calorimeter is used to measure the thermophysical properties of compounds under pressure the calorimetric block is lifted, and the substance to be characterized (mercury, vulcanized rubber) is filled in an open glass ampoule and weighed. Then the ampoule is placed in the sample cell resting on a spring (in order to be positioned in the central active part of the detector zone), where it is in contact with the hydraulic pressurizing fluid (propyl alcohol). The system is completely filled with alcohol, making sure of elimination of any air bubbles, which can affect the accuracy of volume changes during the experiment. After closing the cell, the calorimeter block is moved down, so the cells enter into the cylindrical heat flow detectors.

For studying chemical reactions, the scanning calorimeter was used as a temperature oscillation calorimeter and the high-pressure cells replaced by specially designed reaction cells. These cells allow stirring, different addition profiles for one or two reactants and can accommodate a small optical probe coupled to a miniaturized spectrophotometer (for more details see Ref. [2]).

2.3. Calibration procedures

In the isoperibolic calorimeter, the desired amount of heat (in Joules) and the selected voltage are introduced by the operator via the front panel of LabVIEW software. The power output of the heater is measured on-line, integrated over the time and compared with the required amount of heat. As soon as the two values are equal, a digitally controlled relay stops the current. Concomitantly, the temperature difference between reaction mass temperature, T_R, and the temperature of liquid at the jacket outlet is recorded and the area under the measured peak is calculated. The ratio between the two integrals gives the overall heat transfer coefficient, UA, which is further used to obtain the heat of reaction, ΔH_R.

Calibration of the scanning calorimeter was performed with the melting signal of reference substances, e.g. *n*-octane (−56.76 °C and 180.00 J g^{-1}), *n*-decane (−26.66 °C and 199.87 J g^{-1}), and distilled water (0.01 °C and 335 J g^{-1}) [11,12]. The calorimetric peaks were recorded and integrated to calculate the sensitivity of the calorimeter, which depends on the gain of nanovolt amplifier. The average value of three determinations was considered.

3. Results

3.1. Isoperibolic calorimetry and polymerization reactions

The radical polymerization of acrylamide in aqueous media was chosen as model reaction, since it is reproducible well described in literature. On the other side, it is well known that the aqueous solutions of poly(acrylamide) exhibit high viscosities; the modification of viscosity during the reaction induces large changes in heat transfer coefficient. In this case, the heat of reaction cannot be computed from Eq. (1), which is one of the limitations of reaction calorimetry for polymerization reactions. A typical polymerization run is presented in Fig. 2. The reactor jacket was fixed at the working temperature, the monomer and the solvent charged in the calorimetric vessel and as soon as thermal equilibrium is reached, the solution of $KMnO_4$ is added with the pump. Polymerization does not start in the presence of $KMnO_4$ (the first endothermic peak, noted by digit 1) but starts soon after addition of oxalic acid (the second endothermic peak). The maximum increase of temperature of the reaction mass ($\Delta T_R = T_R - T_{J\_Out}$) was about 7.3 °C. In addition, the stirrer power increases suddenly as soon as the polymerization begins and is maintained at constant level at the end of polymerization.

To quantify the heat of reaction, the correlation between the temperature difference and the corresponding heat flow were determined from (a) the global heat transfer coefficient, UA,

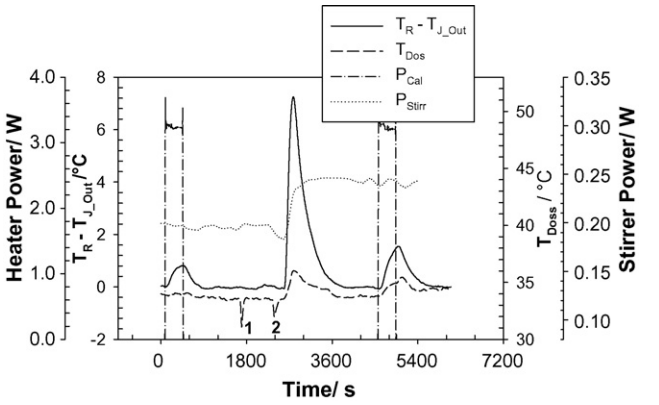

Fig. 2. Acrylamide polymerization at 39 °C with $KMnO_4/H_2C_2O_4$ redox system in 10% aqueous solution. The following data are plotted: temperature difference between reaction mass and liquid at jacket outlet, $\Delta T_R = T_R - T_{J\_Out}$; dosing temperature of initiating system, T_{Doss}; calibration power, P_{Cal}; stirring power, P_{stirr}. For both calibrations the amount of heat dissipated by the calibration element was the same, 1200 J.

which allows the conversion of measured increase of temperature in terms of power (I in Fig. 3); and (b) the determination of calorimeter time constant, τ, and subsequently the deconvolution of thermokinetic data (II in Fig. 3). In the first step, a known amount of power P is dissipated through the calibration heater during a well-defined period, t_{cal}, resulting in a temperature increase. The heat generated during the calibration and the corresponding UA are calculated as follows:

$$Q_c = Pt = UA \int_0^{t_{cal}} \Delta T_R \, dt = UAS^* \rightarrow UA = \frac{Q_c}{S^*} \qquad (2)$$

where S^* is the area of the calibration peak (°C s). After calibration the determination of reaction heat, Q_r, is very easy: $Q_r = UAS$; where S is the integral of reaction effect. The second step, deconvolution of the calorimetric signal, makes use of the calibration signals and implies a differentiation method based on the convolution of the measured $W(t)$ by the generated one $\phi(t)$

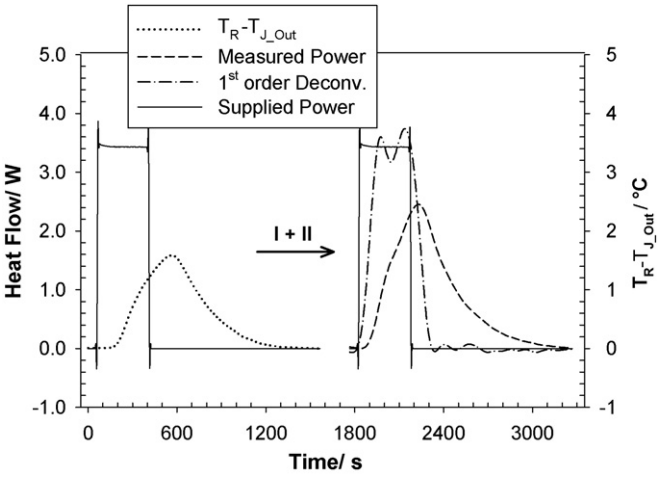

Fig. 3. Effect of global heat transfer coefficient, UA, and of deconvolution on the measured increase of temperature compared with the supplied heat pulse during the calibration.

represented by the following system of linear equations [13]:

$$\phi_1(t) = \phi(t) + \tau_1 \frac{d\phi(t)}{dt}, \qquad \phi_2(t) = \phi(t) + \tau_2 \frac{d(\phi_1(t))}{dt},$$

$$\phi_n(t) = \phi(t) + \tau_n \frac{d\phi_{n-1}(t)}{dt} \ldots \tag{3}$$

where $W(t) = \lim_{n\to\infty}\phi(t)$ and $\tau_1, \tau_2 \ldots \tau_n$ are calorimeter time constants of successive orders. In practical cases, a limited number (usually one) of linear equations is used. The effect of both heat transfer coefficient and first-order deconvolution on the shape of heat measured during a calibration is illustrated in Fig. 3.

Usually, the calibration is performed before and after reaction experiment. When the difference between the areas is significant, as in the case of polymerization reactions, the two values of the heat transfer coefficient are interpolated to obtain the desired $UA(t)$ profile, which is subsequently used for determination of the heat of reaction. The quality of results depends heavily on the interpolation procedure used (i.e. average value, linear with time, proportional to conversion, proportional to the power input of the stirrer). The most important parameters of the polymerization illustrated in Fig. 2 are collected in Table 1. The values obtained for heat of polymerization, ΔH_R, agreed well with the one reported in literature, i.e. 89.6 kJ/mol [14].

The first example concerns the use of reaction calorimetry to increase polymer yield. Oxygen has an inhibiting effect in free radical polymerization and the propagation step is prematurely stopped at relatively low conversions. Solution polymerization of acrylamide was initiated with potassium persulfate, and small amounts of ascorbic acid (aqueous solution) were added. In the presence of ascorbic acid, oxygen traces do not inhibit the process but act as a complementary activator by free radicals formation. The polymerizations were carried out at three temperatures, 40, 50 and 60 °C, respectively, under the presence of atmospheric oxygen (Fig. 4). After the temperature declined to the baseline, the polymerization was reinitialized by alternating addition of potassium persulfate and ascorbic acid.

The second example illustrates how the RC can be used to evaluate the minimal temperature at which an initiating system becomes efficient (Fig. 5). The experiment was carried out

Table 1
Evolution of the global heat transfer coefficients, UA, of the calorimeter time constants, τ, and of heat of polymerization, ΔH_R, in function of the interpolation method used to describe the variation of UA during the polymerization of acrylamide, AM, in water

Measured parameters	Values
Global heat transfer coefficient (UA)	
Before polymerization (UA_1)	3.409 W °C
After polymerization (UA_2)	1.402 W °C
Time constant (τ)	
Before polymerization (τ_1)	92 s
After polymerization (τ_2)	268 s
Heat of reaction (ΔH_R)	88.21 ± 3.4[a] kJ mol^{-1}

Reactions conditions: temperature, 39 °C; initial monomer concentration, 10% (w/w) (aqueous solution); initiator, $KMnO_4/H_2C_2O_4$ redox system.
[a] $n = 8$.

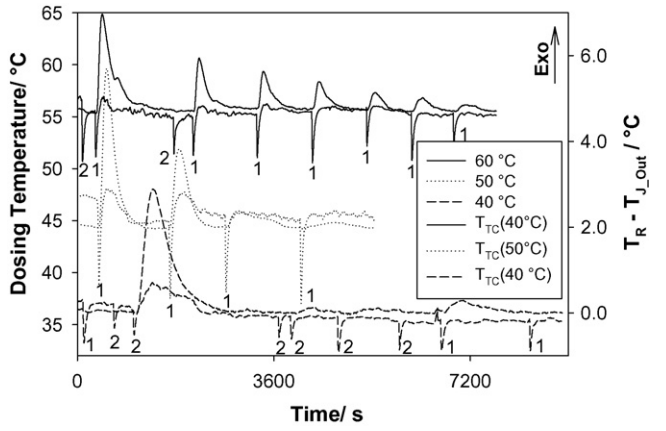

Fig. 4. Acrylamide polymerization at different temperatures with $K_2S_2O_8$/ascorbic acid redox system in 7.5% aqueous solution. The curves with exothermic peaks correspond to the increase of temperature due to the polymerization, while those having endothermic peaks are related to the addition of initiator. The digit '1' denotes the adding of potassium persulfate and the digit '2' the adding of ascorbic acid.

by scanning the temperature from 25 to 53 °C at 0.2 °C/min. After the first calibration, at constant temperature (25 °C), the redox system, potassium persulfate (endothermic peak '1') and ascorbic acid (endothermic peak '2'), are fed into the system. Polymerization starts at about 32.8 °C and the stable dynamic baseline is reached after 18 min, at about 41.2 °C; in this case, the maximal increase of reaction mass temperature, ΔT_R-max, was about 3.5 °C. Subsequent addition of potassium persulfate or ascorbic acid did not restart the polymerization because all monomer was already converted into polymer.

3.2. Temperature oscillation calorimetry

The problem of a correct calorimetric evaluation despite a changing heat transfer coefficient may be solved with temperature oscillation calorimetry (TOC). This technique determines the heat transfer coefficient during the reaction from forced temperature oscillations [15]. The Calvet-type differential calorimeter was used to perform TOC measurements. The

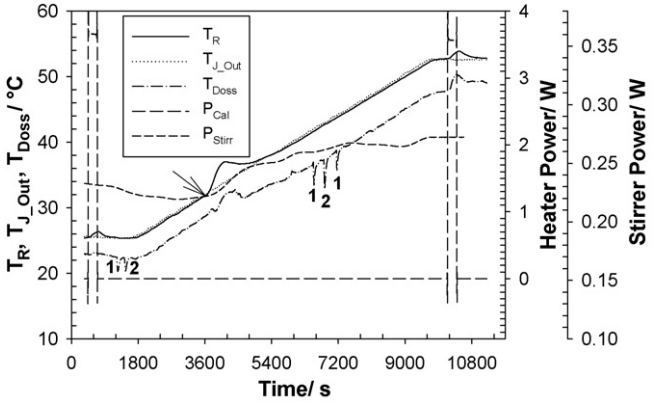

Fig. 5. Plots of raw data acquired during acrylamide polymerization in temperature programmable ramp mode with potassium persulfate/ascorbic acid redox system.

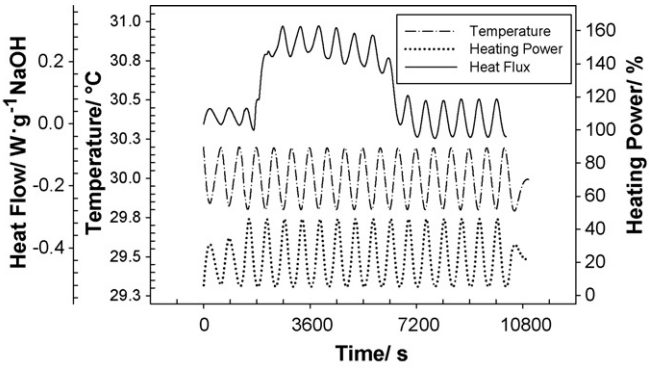

Fig. 6. Heat flow, temperature of the calorimetric block, and power output of the heating elements during the neutralization reaction at 30 °C.

desired oscillations of temperature were obtained by imposing a sinusoidal variation of the set-point of calorimetric block by means of an external temperature control system.

The evaluation of energy balance [Eq. (1)] is performed in two steps. In the first step the heat transfer value *UA* is calculated from temperature oscillations. In the second step the reactor energy balance without oscillating heat contribution is considered and the chemical heat flow, Q_{Chem}, is calculated from Eq. (1). Given that Eq. (4) is the general expression for an oscillating signal, and considering only the influence of oscillating terms on energy balance the equations for *UA* [Eq. (5)] and heat capacity C_P [Eq. (6)] are obtained [16]:

$$X = A_x \, e^{i(\omega t + \varphi x)} \tag{4}$$

$$UA = \frac{A_Q}{A_T} \cos(\varphi_Q - \varphi_T) \tag{5}$$

$$mc_p = \frac{A_Q}{\omega A_T} \sin(\varphi_Q - \varphi_T) \tag{6}$$

The values of phase and amplitude for each signal during the course of chemical reaction can be obtained by applying a Fourier transform to each measured signal.

The neutralization reaction of H_2SO_4 (0.5 N) with NaOH (0.5 N) was selected as model reaction ($-139.1\ \text{kJ mol}^{-1}$). The addition period of NaOH was 80 min. The raw data of a typical run are plotted in Fig. 6. The reaction conditions were: reaction temperature 30 °C, the amplitude of temperature oscillations 0.25 °C, the period of oscillation 10 min, and the temperature of the cooling liquid in the jacket of the calorimetric block

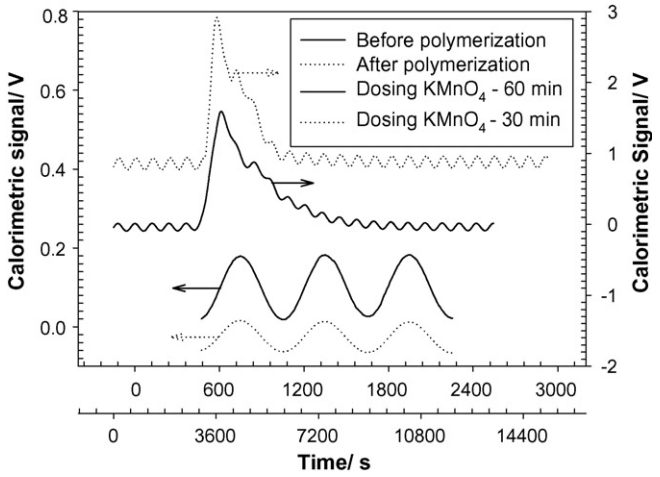

Fig. 8. Heat flow evolution during the solution polymerization of acrylamide at 40 °C with $KMnO_4/H_2C_2O_4$. The dosing periods of $KMnO_4$ were 60 min (full line) and 60 min (dotted line), respectively. In the lower part of figure the amplitude of the calorimetric signal before and after polymerization is illustrated.

0 °C. After mathematical treatment of the raw data both the heat transfer coefficient, *UA*, and heat of neutralization, Q_{Chem} are obtained (Fig. 7). As expected, the overall heat transfer coefficient, *UA*, increases almost linearly during the experiment (Fig. 7(a)), since the wetted surface area in the reactor, *A*, increases during the dosing period. Thus, the *UA* increases from 17 to about $35\ \text{W °C}^{-1}$ during the dosing period and the integration of heat released during the neutralization gives an enthalpy of $-133.5\ \text{kJ mol}^{-1}$ which is close to the literature values.

TOC was also applied to the polymerization of acrylamide (7.5% aqueous solution). In this case, the reaction temperature was 40 °C, the amplitude of temperature oscillations 0.25 °C, the period of oscillation 10 min, and the temperature of the cooling liquid in the jacket of the calorimetric block 10 °C. In a typical experiment the reaction cell contained 4 ml aqueous solution of acrylamide and the corresponding amount of oxalic acid (30 μl aqueous solution 10%, w/w). After thermal equilibrium, the temperature oscillation is imposed and after 6 periods, the solution of the second redox initiator ($KMnO_4$, 50 μl aqueous solution 5%, w/w) is fed over a period. As Fig. 8 shows, the feeding period of $KMnO_4$ controls both the amplitude and the span of calorimetric peak, i.e. the rate of polymerization at a given temperature, with increasing amount in the reaction mass the polymerization rate

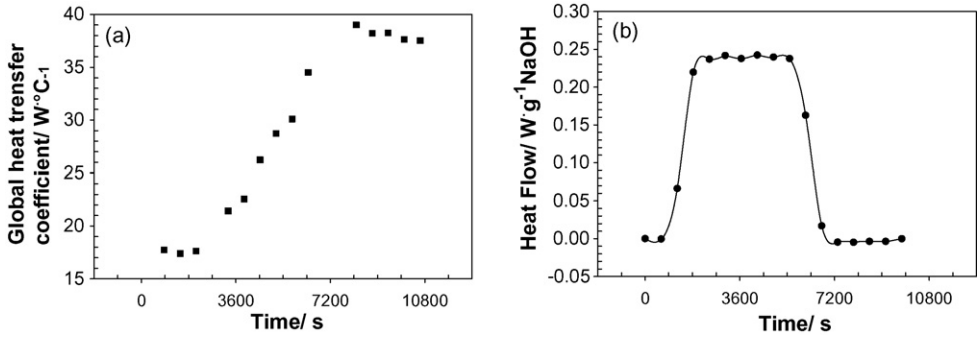

Fig. 7. Heat transfer (a) and heat flow (b) evolution during the neutralization reaction at 30 °C.

increase. As is seen in the lower part of Fig. 8, the decrease of amplitude of raw calorimetric signal from 0.1 to about 0.0375 V due to the large increase of viscosity during the solution polymerization, which, in turn, induces the decrease of heat transfer coefficient.

3.3. Low temperature–high pressure phase transitions

Performing high-pressure, low-temperature *pVT*-calorimetry is a challenge. The performance of the scanning transitiometer–cryostat were discussed in detail in Ref. [17]. Briefly, during isothermal runs, the calorimeter temperature is selected first, depending on the phase transition temperature of investigated sample, and the temperature of cooling fluid (cryostat) is programmed to be 20 °C below the calorimeter temperature. In this way the electronic heater control enables an extremely stable temperature during the experiment, i.e. the stability of temperature is better than ±1 mK. For fusion under isothermal conditions, the pressure was continuously decreased into the pre-established range (e.g. 100–10 MPa). The scanning rates ranged from 0.2 to 1 MPa min^{-1}, the typical value being 0.4 MPa min^{-1}. For isobaric runs the temperature program of calorimetric block was combined with the cryostat program to assure an stable temperature gradient during temperature scanning experiments. This mode induces a very stable baseline of the heat flow signal with a minimum of noise. Thus, during the fusion runs the temperature of the cooling–heating fluid was always lower than that of the calorimetric block during the equilibration periods (isothermal segments) and it was higher, with a gradient of 20 °C, during the dynamic segment. Just before the beginning of scanning temperature, the temperature of heating-cooling device jumps rapidly (in 5 min) and runs in parallel with the temperature of calorimetric block. In such a way, the scanning rate could be increased to 0.6–0.7 °C min^{-1}, which is about twice the maximal scanning rate with this type of calorimeter without the heating fluid; in most experiments the scanning rate was 0.4 °C min^{-1}.

To illustrate the performance of scanning transitiometry at low temperature and high pressure mercury was selected as model substance for first order phase transition (fusion) and some polymeric materials for pseudo-second order phase transition (glass transition temperature), respectively.

Table 2
Pressure dependence of the mercury fusion temperature, associated volume changes, and enthalpy of fusion

Pressure (MPa)	T_{onset} (°C)	$\Delta_{fus}V_{spec}$ ($\times 10^{-3}$ cm^3 g^{-1})	$\Delta_{fus}H$ (J g^{-1})
15	−38.285	2.491	11.456
30	−37.389	2.451	11.466
50	−36.366	2.423	11.470
70	−35.536	2.411	11.483
90	−34.412	2.398	11.498

3.3.1. Fusion of mercury

The data obtained by scanning transitiometry concerns the effect of pressure, in the pressure range from 0.1 to 100 MPa, on the latent heat of fusion of mercury. The experiments were performed both at constant pressure (by scanning temperature) and under isothermal conditions (by scanning pressure).

The pressure effect on the melting of mercury is illustrated by five calorimetric plots obtained at 15, 30, 50, 70, and 90 MPa in Fig. 9(a) and the simultaneously recorded volume changes associated to the mercury fusion and are plotted in Fig. 9(b). The melting temperature, T_{onset}, is shifted toward higher temperatures with increasing the pressure. In this figure the fusion peaks obtained at 70 and 90 MPa seem to be more intense, but this is because the amplifier gain was increased from 1501 to 3401, respectively. The enthalpy of fusion slightly increases with pressure (Table 2).

The melting temperature as a function of temperature gives a straight line with a slope of 0.0504 ± 0.005 °C MPa. The volume changes associated of mercury fusion were simultaneously recorded and are plotted in Fig. 9(b). There is a good accordance between the effect of pressure on the transition temperatures measured by enthalpy of fusion and volume change [17]. The pressure dependence of the heat of fusion of mercury may be estimated from the heat flow data as:

$$\Delta_{fus}H = \Delta_{fus}H_0 - (3 \pm 2.2)10^{-4}p + (7.529 \pm 2.342)10^{-6}p^2 \quad (7)$$

where p is the pressure in MPa and $\Delta_{fus}H_0 = 11.469 \pm 0.008$ J g^{-1} at normal pressure [18]. The enthalpy of fusion increases somewhat with pressure; this increase is less than 0.5% per 100 MPa in the investigated range of pressure.

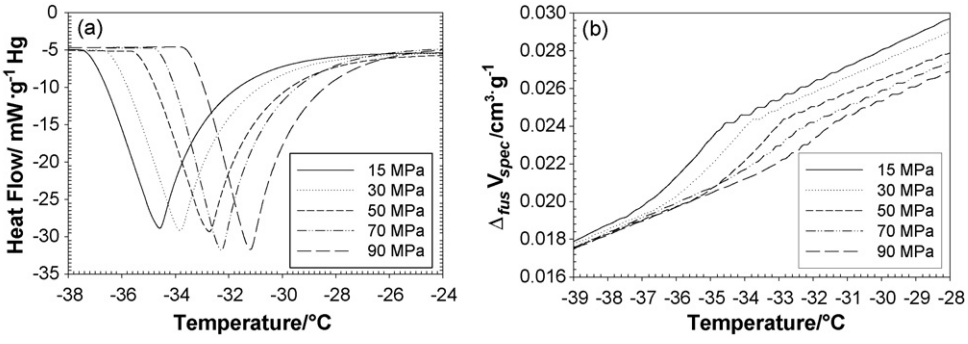

Fig. 9. Effect of pressure on the mercury fusion under isobaric conditions: (a) thermograms of mercury fusion and (b) associated volume variation, ΔV. The scanned interval of temperature was between −60 and −10 °C at a scanning rate of 0.4 °C min^{-1}.

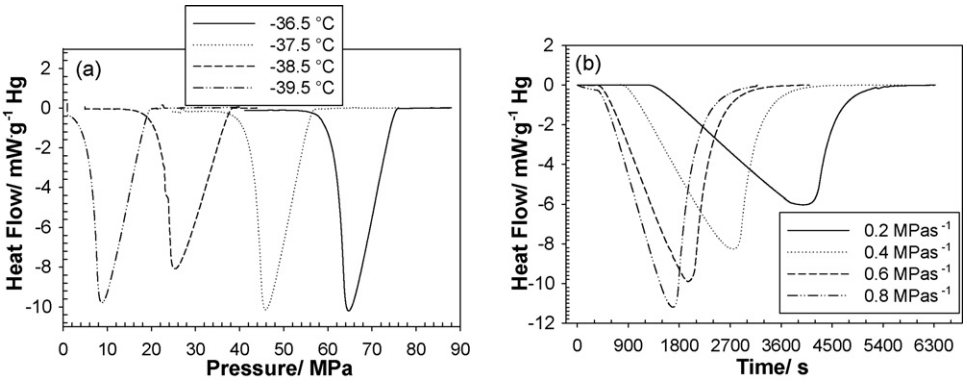

Fig. 10. Effect of pressure on mercury fusion under isothermal conditions: (a) thermograms of mercury fusion and (b) as function of pressure scanning rate at −38.5 °C.

Table 3
The main characteristics of mercury fusion peaks obtained during isothermal pressure scans (decompression)

Variable	p_{onset} (MPa)	$\Delta_{fus}H$ (J g^{-1})
Temperature (°C)		
−39.5	18.883	11.419
−38.5	37.682	11.396
−37.5	56.120	11.448
−36.5	74.993	11.502
Pressure scanning rate (MPa min^{-1}) at −38.5 °C		
0.2	38.364	
0.4	37.704	11.40 ± 0.018
0.6	37.336	
0.8	36.828	

Four calorimetric plots at temperatures ranging from −36.5 to −39.5 °C are presented in Fig. 10(a). The pressures corresponding to the phase change increase with increasing the temperature. The main characteristics of the fusion peaks are given in Table 3.

The heats of fusion evaluated by integrating the calorimetric peaks are in fairly good accord with literature data at normal pressure [18]. The temperature dependence of the pressures corresponding to the onset of mercury fusion gives a straight line with the regression Eq. (8):

$$p_{fus} = (18.0154 \pm 0.366)T + 755.6 \pm 14.497 \quad (8)$$

where T is the working temperature in °C. Extrapolation to the ordinate gives the value of 755.6 MPa which is in good agreement with the value found by Johnson and Newhall, 756.8 MPa, for mercury at 0 °C [19].

The impact of the pressurization rate appears clearly in Fig. 10(b). As this figure shows, when represented as a function of time, the peak height increases and peak span decreases with increasing pressurization rates.

3.3.2. Glass transition temperature of vulcanized rubber

DSC detects the glass transition as a change in the heat capacity as the polymer matrix goes from the glass state to the rubber state, so the transition appears as a step transition and not a peak such as might be seen with a melting transition. An increased pressure causes an expected increase in T_g based on the prediction of decreased free volume. This result is important in engineering operations such as molding or extrusions, when operation too close to T_g can result in a stiffening of the material. Investigation of the glass transition of polymers under pressure is difficult especially where T_g is well below ambient temperature. The effect of the temperature scanning rate on the intensity of phase transition is illustrated in Fig. 11. As expected, both T_g and the amplitude of phase transition increase with increasing the temperature scanning rate.

Fig. 12(a) shows the evolution of T_g at different pressures, i.e. 10, 30, 50, 70, and 90 MPa. T_g increases linearly with pressure with a slope of 0.193 ± 0.002 K MPa^{-1}. It should be noted that

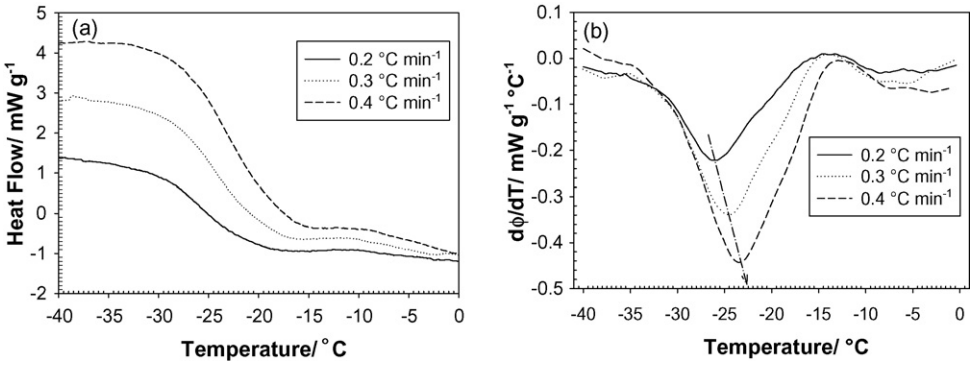

Fig. 11. Effect of temperature scanning rate on the amplitude and glass transition temperature: (a) heat flux curves and (b) derivatives with respect to temperature of heat flow curves. The scanned interval of temperature was −60 to +10 °C.

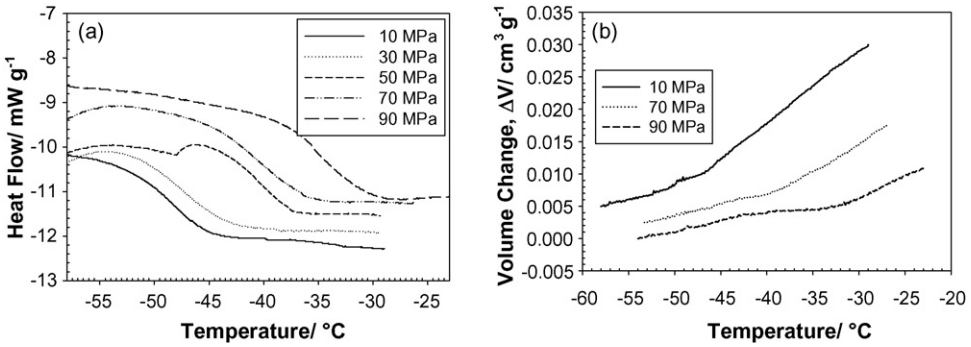

Fig. 12. Effect of pressure on the vulcanized rubber glass transition temperature under isobaric conditions: (a) heat flux evolution and (b) associated volume variation, ΔV. The scanned interval of temperature was −70 to −10 °C at a scanning rate of 0.4 °C min^{-1}.

T_g is expressed as the temperature corresponding to the peak of the first derivative of the heat flow (i.e. the inflection point on the heat flow curve). The associated volume variations with the glass transition are depicted in Fig. 12(b). In accord with the heat flow curve, the T_g increases with increasing the pressure. Above the glass transition temperature there is an increase to the slope of the specific volume versus temperature. However, the change in the slope is gradual and T_g can be determined by locating where the two lines intersect.

4. Conclusions

TOC allows to obtain on-line parameters involved in the heat balance of the reaction mass during a chemical reaction. A good behaviour in the response of the system at different oscillation parameters was obtained, with reliable results in the determination of reaction power of polymerization reactions. In addition, it was proved that a simple isoperibolic RC can be successfully used to increase the yield or to asses the efficiency of initiators in the near-to-the-industrial condition if special attention is paid to the baseline determination, i.e. change of global heat transfer coefficient during the process, and to the deconvolution of measured heat flow.

In order to characterize the thermophysical properties of compounds under pressure at low temperature a scanning transitiometer was coupled with a computer controlled cryostat Reproducible measurements were obtained with this setup and the resulting phase transition parameters are in good agreement with literature values, for both first order phase transition (mercury fusion) and second order phase transition (rubber glass transition temperature) in a pressure range from 10 to 100 MPa and at temperatures starting from −70 °C. The main advantage of scanning transitiometry is the possibility of concomitant recording both of the heat flow and the volume variations associated to the phase transition. The data furnished by the two techniques are complementary to each another and their critical analysis allows a more accurate interpretation of the phase transition phenomenon.

Acknowledgements

The authors are grateful to the Romanian Ministry of Education and Research and to the French Embassy in Romania for the financial support in the mark of Programme d'Actions Intégrées - Brancusi (VJ0889). Thanks are due also to M. Chabut, G. Petrescu, and J.-F. Verdier for their help in performing calorimetric measurements.

References

[1] J. Pastré, A. Zogg, U. Fischer, K. Hungerbühler, Org. Process Res. Dev. 5 (2001) 158–166.
[2] F. Dan, J.-P.E. Grolier, in: T. Letcher (Ed.), Chemical Thermodynamic for Industry, Royal Society of Chemistry, Cambridge, 2004, pp. 88–103.
[3] P.G. De Luca, C. Scali, Chem. Eng. Sci. 57 (2002) 2077–2087.
[4] L. Bou-Diab, B. Schenker, I. Marison, S. Ampuero, U. von Stockar, Chem. Eng. J. 81 (2001) 113–127.
[5] M. Lathi, A. Avela, J. Seppälä, Thermochim. Acta 262 (1995) 33–43.
[6] J.-P. Grolier, F. Dan, S.A.E. Boyer, M. Orlowska, S.L. Randzio, Int. J. Thermophys. 25 (2) (2004) 297–319.
[7] G.W.H. Höhne, Thermochim. Acta 332 (1999) 115–123.
[8] H.J. Jin, X.J. Gu, P. Wen, L.B. Wang, K. Lu, Acta Mater. 51 (2003) 6219–6231.
[9] F. Dan, J.-P.E. Grolier, Proceedings of the 14th Romanian International Conference on Chemistry and Chemical Engineering (RICCCE 14), vol. S09, Bucharest, September, 2005, pp. 150–157.
[10] J.-P.E. Grolier, F. Dan, S.A.E. Boyer, M. Orlowska, S.L. Randzio, Int. J. Thermophys. 25 (2) (2004) 297–319.
[11] S. Stølen, F. Grønvold, Thermochim. Acta 327 (1999) 1–32.
[12] N.S. Osborne, J. Res. Natl. Bur. Stand. 23 (1939) 643–646.
[13] L. Vincent, N. Sbirrazuoli, S. Vyazokin, Ind. Eng. Chem. Res. 41 (2002) 6650–6655.
[14] J. Brandurp, E.H. Immergut (Eds.), Polymer Handbook, John Wiley & Sons Inc., New York, 1975, p. 273.
[15] A. Tietze, I. Ludke, K.-H. Reichert, Chem. Eng. Sci. 51 (11) (1996) 3131–3137.
[16] J. Sempere, R. Nomen, E. Serras, J. Sales, J. Therm. Anal. Calorim. 52 (2003) 65–71.
[17] F. Dan, J.-P.E. Grolier, Thermochim. Acta 446 (2006) 73–83.
[18] J.E. Callanan, K.M. McDermott, E.F. Westrum, J. Chem. Thermodyn. 22 (1990) 225–230.
[19] D.P. Johnson, D.H. Newhall, Trans. Am. Soc. Mech. Engrs. 75 (1953) 301.